Extreme precipitation driven by the rapid tropical Atlantic warming and the second developing La Niña over the Yangtze–Huaihe River Basin in August 2021

Junhu Zhao[1,2] · Jinqing Zuo[1,2] · Han Zhang[3] · Lijuan Chen[1,2] · Jie Yang[4] · Zheng Zhihai[1] · Guolin Feng[1]

Abstract

In 2021, the Yangtze–Huaihe River Basin (YHRB) of China underwent normal precipitation during the classical Meiyu period in June–July but suffered extreme precipitation and severe floods in August. The present study revealed that the extreme heavy precipitation anomalies over the YHRB region were closely related to the combined effect of the strong western North Pacific anomalous anticyclone (WNPAC) and East Asian middle–high latitude circulation anomalies in August 2021. Moreover, the background of sea surface temperature (SST) anomalies was a strong eastern-Pacific La Niña event that rapidly decayed in spring and a second La Niña emerged in late summer, accompanied by a weak tropical Indian Ocean warming and a strong tropical Atlantic warming in summer. The rapidly decaying La Niña event and the weak tropical Indian Ocean warming alone seem to be insufficient to induce the strong WNPAC in August 2021. Observational evidence and numerical experiments suggest that the rapid tropical Atlantic warming from late spring to summer observably contributed to the enhancement and westward shift of the WNPAC, and the cold SST anomalies in the eastern tropical Pacific associated with the second La Niña event also provided favorable conditions for a strong WNPAC in August 2021. Overall, rapid tropical Atlantic warming and the development of the second La Niña contributed to the strong WNPAC in August 2021, while the maintenance mechanism of the East Asian middle–high latitude circulation anomalies that controlled cold air activity remains unclear.

Keywords Extreme precipitation over the Yangtze–Huaihe River Basin · WNPAC · La Niña · Tropical Atlantic · East Asia cold air activity

1 Introduction

Meiyu (Baiu in Japan, and Jangma/Changma in Korea) is the major and unique rainy season controlled by the East Asian summer monsoon (Ninomiya and Muraki 1986; Tao and Chen 1987; Ding 1992). It generally refers to the consecutive precipitation and high temperature weather in early summer over the Yangtze River–Huaihe River Basin (YHRB) of China, which accounts for 30–40% of the average annual precipitation in that region (Wu et al. 2006; Ding et al. 2020). The duration and intensity of Meiyu exhibit high interannual variability, leading to a high frequency of drought/flood events in the YHRB (He et al. 2007; Zhao et al. 2018a, b; Li et al. 2019). For example, the Meiyu intensity was strong, and thus, the YHRB experienced heavy floods in the summers of 1998, 2016 and 2020 (Li 1999; Zhao et al. 2018a, 2021). Especially in the summer of 2020,

✉ Jinqing Zuo
zuojq@cma.gov.cn

✉ Lijuan Chen
chenlj@cma.gov.cn

1. China Meteorological Administration Key Laboratory for Climate Prediction Studies, National Climate Center, Beijing 100081, China

2. Collaborative Innovation Center On Forecast and Evaluation of Meteorological Disasters (CIC-FEMD), Nanjing University of Information Science and Technology, Nanjing 210044, China

3. School of Atmospheric Sciences and Guangdong Province Key Laboratory for Climate Change and Natural Disaster Studies, Sun Yat-Sen University, Zhuhai 519000, China

4. Jiangsu Climate Center, Nanjing 210008, China

the longest Meiyu season occurred over the past sixty years (Ding et al. 2021; Zhang et al. 2021; Qiao et al. 2021), and the associated significant flooding affected approximately 45.5 million people and caused a direct economic loss of more than 100 billion Chinese Yuan (Wei et al. 2020).

In June–July 2021, the intensity of Meiyu was normal (Zhao et al. 2022a). In August 2021, however, the YHRB region experienced prolonged heavy precipitation and extensive flooding, and the regionally averaged precipitation for the basin was 227 mm, which was 58.7% higher than the climatological mean precipitation in August for the period of 1981–2010 and set the highest record since 1981. These anomalously long-lasting precipitation and heavy flooding events have caused significant impacts. Hence, the sustained heavy precipitation that occurred in August was referred to as "Dao huang mei" weather by the media and the public in China, denoting the second Meiyu period in late summer. Therefore, it is important to explore the causes of the remarkable subseasonal variation in the YHRB precipitation anomalies in the early and late summer of 2021. Zhao et al. (2022a) showed that the western North Pacific (WNP)–East Asian atmospheric circulation experienced remarkable subseasonal changes between June–July and August in 2021; that is, the western North Pacific anomalous anticyclone (WNPAC) was normal in June–July but became stronger than normal in August, leading to weaker Meiyu in June–July and stronger "Dao huang mei" weather in August. Concurrent with this evident subseasonal change, the central–eastern tropical Pacific Ocean (TPO) featured a decaying La Niña event in spring and a second developing La Niña in the eastern tropical Pacific in late summer, while sustaining weak sea surface temperature (SST) warming occurred in the tropical Indian Ocean (TIO). However, previous studies have demonstrated that La Niña decaying summers generally witness an anomalous low-level cyclone over the WNP (Wu et al. 2010; Tao et al. 2017; Feng et al. 2017; Wang et al. 2019b). Then, questions arise concerning what caused the strong WNPAC and thus heavy precipitation over the YHRB region in August 2021.

Numerous studies have shown that the WNPAC plays a vital role in influencing the extreme weather and climate in the western Pacific–East Asian region. The WNPAC strongly affects moisture transport and precipitation anomalies over East Asia by modulating monsoon variability and tropical cyclone activities (Wang et al. 2013; Li et al. 2017; Zhao et al. 2021, 2022b). Over the past decades, extensive studies have focused on the physical mechanisms for the formation and maintenance of the WNPAC (see review papers by Li and Wang 2005; Li et al. 2017), which involves ENSO-related Indo-Pacific SST forcing (e.g., Zhang et al. 1996; Wang et al. 2000; Xie et al. 2009, 2018; Wu et al. 2017a, b) and remote forcing of tropical Atlantic (TA) SST anomalies (Rong et al. 2010; Hong et al. 2014, 2015; Zuo et al. 2019).

The WNPAC, persisting from the developed El Niño winter to the subsequent summer, is a predominant connection of El Niño and the East Asian summer monsoon (Chang et al. 2000; Wang et al. 2000; Li et al. 2007; Chen et al. 2012). Wang et al. (2000) showed that the WNPAC is generated as a response to El Niño heating over the central–eastern TPO and maintained by local air–sea interactions. Furthermore, the warming SST anomalies (SSTAs) over the TIO, following the winter El Niño events, contribute to the persistence of the WNPAC by inducing an eastward atmospheric Kelvin wave (e.g., Xie et al. 2009, 2016). Therefore, these studies demonstrated that El Niño and the associated TIO warming play an important part in forming and maintaining the strong WNPAC. However, the physical mechanisms driving the extremely strong WNPAC in August 2021 during a La Niña decaying phase remain unclear. Hence, we revisit the possible mechanism for the subseasonal change in the WNPAC in summer 2021 through observational analysis and numerical simulations.

The rest of this paper is organized as follows. The data and methods are described in Sect. 2. Subseasonal changes in the YHRB precipitation anomalies and associated circulation anomalies in summer 2021 are presented in Sect. 3. In Sect. 4, the evolution of SSTAs during 2021 and their influence on the subseasonal changes in the WNP–East Asian atmospheric circulation using both observations and numerical modeling experiments are explored. Finally, Sect. 5 contains a summary and some discussion on the impact of the Madden–Julian Oscillation (MJO).

2 Datasets, methodology, and numerical experiments

2.1 Datasets and method

In this study, we used daily precipitation data from 2400 stations provided by the National Meteorological Information Center of China (Ren et al. 2012), and the combined precipitation data from monthly mean Global Precipitation Climatology Project (GPCP; Adler et al. 2018), which have been gridded at $2.5° \times 2.5°$ since 1979. Atmospheric variables are obtained from the NCEP/NCAR reanalysis gridded at $2.5° \times 2.5°$ (Kalnay et al. 1996) and available from 1948 to the present. The monthly outgoing longwave radiation (OLR) is obtained from the NOAA Interpolated OLR dataset (Liebmann and Smith 1996), which has been gridded at $2.5° \times 2.5°$ since 1974. The SST data are obtained from the Hadley Centre Sea Ice and Sea Surface Temperature (HadISST, Reynolds et al. 2002), which has been gridded at $1.0° \times 1.0°$ since 1870. The daily real-time multivariate MJO (RMM) indices (Wheeler and Hendon 2004) are available

from the Australian Bureau of Meteorology (http://www.bom.gov.au/climate/mjo/).

The Niño3.4, TIO and TA SST indices are defined as the averaged SSTAs over the region (120°–170° W, 5° S–5° N), (40°–110° E, 10° S–20° N) and (70° W–0°, 5° S–5° N), respectively. The WNPAC index is defined as the averaged stream function at 850 hPa over the region (10°–25° N, 110°–155° E), where the WNPAC variability is strong in summer (Zuo et al. 2019). Following Zhang et al. (2018), the position of the East Asian subtropical westerly jet (EASWJ) is represented as the difference in the 200-hPa zonal wind between (37.5°–42.5° N, 90°–130° E) and (32.5°–37.5° N, 90°–130° E) in June, between (40°–45° N, 90°–130° E) and (35°–40° N, 90°–130° E) in July, and between (42.5°–47.5° N, 90°–130° E) and (37.5°–42.5° N, 90°–130° E) in August. The positive (negative) index represents a northward (southward) shift of the EASWJ.

In this paper, the anomaly fields are obtained relative to climatology during the period of 1981–2010. The statistical significance of correlation coefficients, regression and the ensemble-mean differences of model outputs are evaluated using a two-tailed Student's *t* test.

2.2 Model and experimental setup

The Community Atmospheric Model version 5.3, which is an atmospheric general circulation model developed by NCAR (CAM5.3; Hurrell et al. 2013), is used in this study. This model has been widely used to validate the impact of tropical SSTAs on the WNP large-scale atmospheric circulation and East Asian precipitation anomalies during summer (e.g., Ren et al. 2017, 2021; Li et al. 2018; Zuo et al. 2019; Liu et al. 2022). It has a resolution of 1.9° in latitude, 2.5° in longitude and thirty levels in the vertical direction. Three sensitivity experiments are designed to assess the contribution of SSTAs in the tropical Atlantic (TA2021 run), the tropical Pacific Ocean (TPO2021 run) and their combinations (TA + TPO2021 run). Each sensitivity experiment contains fifty ensemble members that are integrated from May 1 to August 31 with slightly varying atmospheric initial conditions. The model outputs in May of each run are discarded as spin-up, and outputs from June to August are used. The ensemble mean of the fifty members is used in the analysis.

The underlying boundary forcings are the observed monthly SSTAs plus the monthly climatological mean SST in the forced region (Table. 1). SSTAs in the forced region are set as 1.5 times the observations in the sensitivity experiments due to the insufficient simulation of the general circulation model of observed atmospheric circulation anomalies (Kang et al. 2002; Hong et al. 2015). In the control run, the model is forced with prescribed monthly climatological means of SST and sea ice that are obtained from the HadISST data, and runs continually for 60 years. The first 10-years are discarded as spin-up. More details of the sensitivity experiments are described in Sect. 4.2.

3 Precipitation and circulation anomalies in summer 2021

3.1 Precipitation anomalies over the YHRB region

The spatial distributions of precipitation anomalies over East China in June–July and August 2021 are presented in Fig. 1a, b, respectively. Apparent differences in precipitation anomalies are observed between June–July and August in the YHRB region. In June–July, the precipitation anomaly was nearly normal in most parts of the YHRB region, except in the eastern part (Fig. 1a). In August, however, the precipitation anomaly became positive and was obviously higher than normal in most parts of the YHRB region (Fig. 1b).

To further investigate the interannual variation in the YHRB precipitation anomalies, we selected 539 stations in the YHRB region (28°–34° N, 105°–122.5° E; black box in Fig. 1a) and constructed the YHRB precipitation index (YHRBPI) averaged over those 539 stations since 1981 (Fig. 1c). The regionally averaged precipitation was 418 mm in June–July 2021 and the anomaly was 0.32 times the standard deviation. Notably, that the precipitation anomalies for most stations over the YHRB region were less than their climatological mean after the precipitation amount induced by typhoons in June–July 2021 were removed, especially Typhoon In-Fa, which listed the longest overland retention time since 1949 (Zhao et al. 2022a). In contrast, the regionally averaged precipitation over the YHRB region reached

Table 1 Scheme design for the numerical experiments

Experiment name	Underlying boundary forcings
CTL	Monthly climatological mean SST and sea ice
TA2021	Attach monthly warm SSTA in the TA (10° S–60° N, 70° W–0°) in May–August 2021 on the SST in the CTL
TPO2021	Attach monthly La Niña-like cold SSTA in the tropical Pacific (20° S–20° N, 150° E–80° W) in May–August 2021 on the SST in the CTL
TA + TPO2021	Attach SSTA in the TA and TPO on the SST in the CTL

(a) Prec anom in JJ 2021

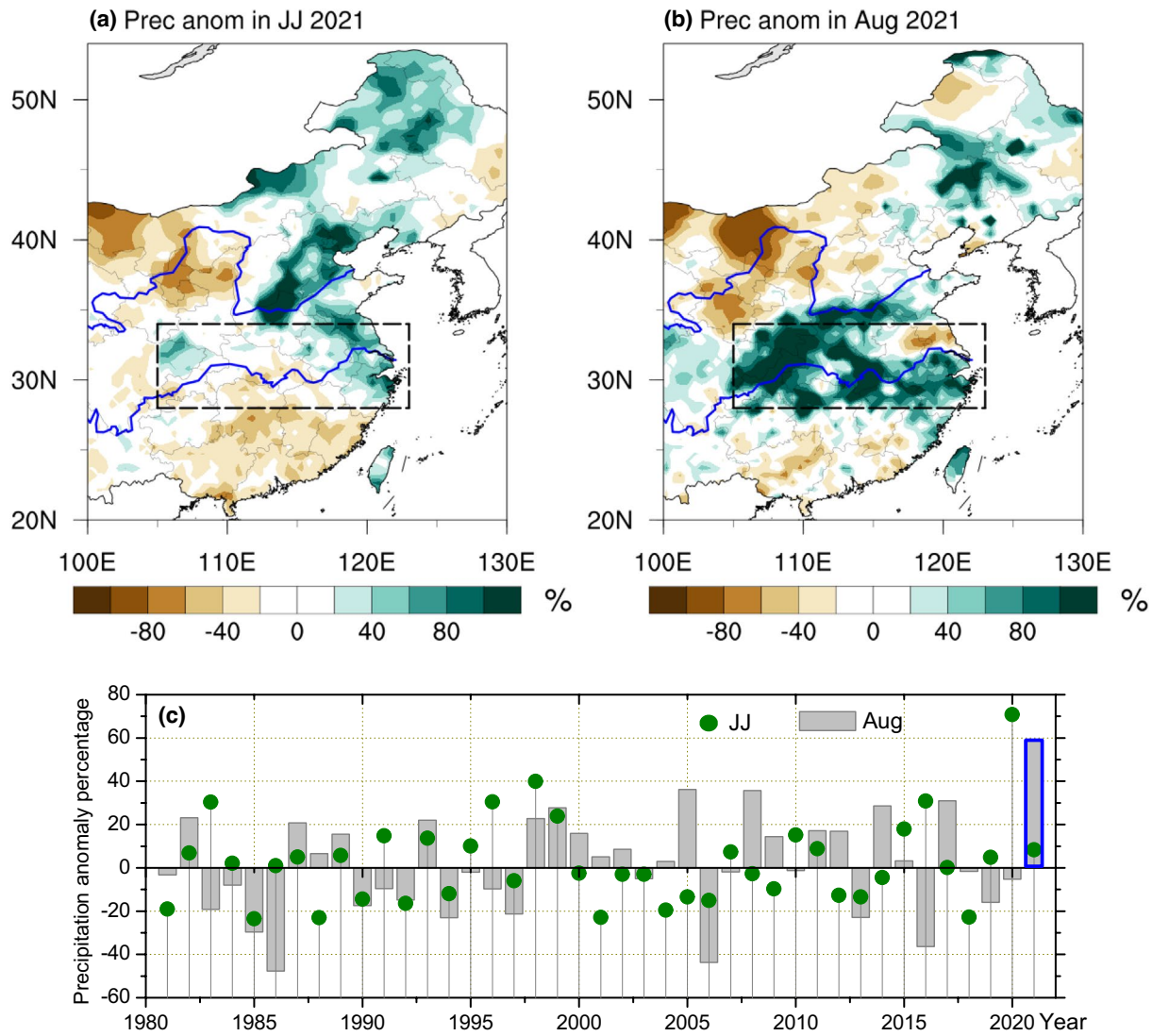**(b)** Prec anom in Aug 2021

Fig. 1 Precipitation anomaly in **a** June–July (JJ) and **b** August 2021. **c** Time series of the regionally averaged precipitation anomaly percentage (unit: %) over the YHRB in JJ (green dots) and August (gray bars) during the period of 1981–2021

227 mm in August 2021 and the anomaly was 2.5 times the standard deviation, leading to the wettest August since 1981.

Figure 2 displays the features of the daily precipitation over the YHRB region during June–July and August 2021. The ratio of daily precipitation (gray bars) exceeding its climatology (blue dots) was approximately 45.9% (28 out of 61 days) in June–July 2021 (Fig. 2a), which was far less than that in June–July 2020 (52 out of 61 days; Zhang et al. 2021). In contrast, the daily precipitation exceeded its climatology for most days in August 2021 (21 out of 31 days) (Fig. 2b). In particular, 8 heavy precipitation

events occurred over the YHRB region in August 2021, leading to several devastating floods in that region.

3.2 Large-scale atmospheric circulation anomalies

Figure 3 displays the subseasonal changes in the large-scale atmospheric circulation anomalies in summer 2021. There is a notable difference in the atmospheric circulation anomalies over the WNP–East Asian region between June–July and August. In June–July, an East Asia–Pacific (EAP)-like pattern was observed in the lower troposphere,

Fig. 2 Daily precipitation (bar; mm/day; left vertical axis) and daily accumulated precipitation (pink line; mm; right vertical axis) over the YHRB (red box in Fig. 1a) **a** from June 1 to July 31 of 2021 and **b** from August 1 to August 31 of 2021. Orange dots and the green line express climatological daily precipitation (mm/day, left vertical axis) and climatological daily accumulated precipitation (mm, right vertical axis), respectively. The blue dots represent the accumulated precipitation (mm; right vertical axis) in all other years (from 1981 to 2020)
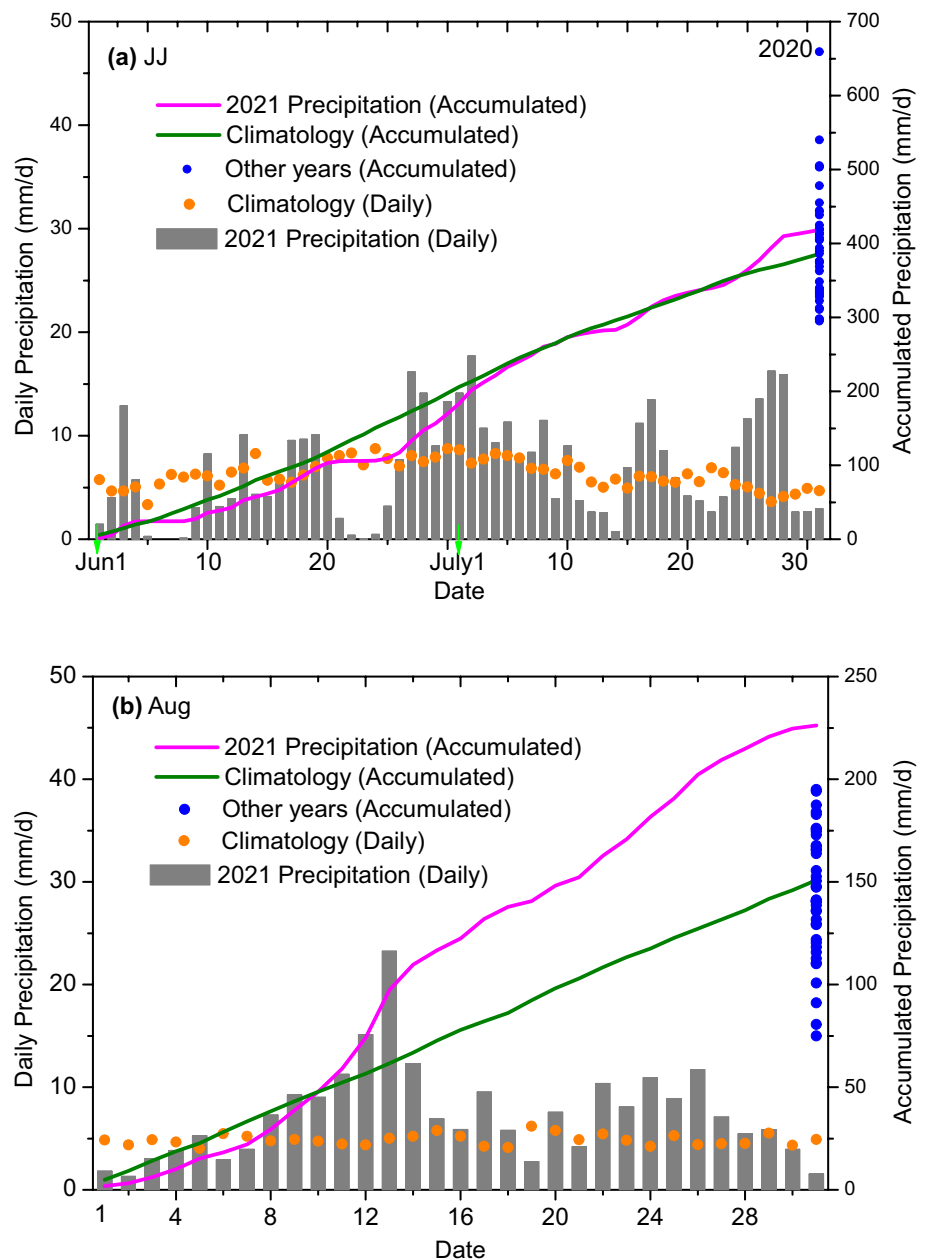
accompanied by an anomalous cyclone over the WNP and an anomalous anticyclone over Northeast Asia (Fig. 3a), leading to intensified water vapor transport from the ocean into northeast China (Fig. 3b) and thus heavy (light) precipitation anomalies in northeastern China (the YHRB region) (Fig. 1a). In August 2021, however, strong low-level anticyclonic anomalies occurred over the WNP (Fig. 3e), indicating an intensified WNPAC. As shown in Fig. 4a, the WNPAC index in August 2021 was 1.51 times of its standard deviation and ranked the third in intensity since 1981, while the index was normal in June–July 2021. Therefore, the intensified WNPAC in August 2021 induced water vapor transport along its western flank from the

tropical ocean into the YHRB region (Fig. 3f), providing favorable conditions for the heavy precipitation anomalies in that region (Fig. 1b).

In addition to the water vapor transport along the western flank of the WNPAC, cold air activity over the Eurasian middle–high latitudes is also very important to the precipitation anomalies over the YHRB region during summer (Tao and Chen 1987; He et al. 2007). In August 2021, negative geopotential height anomalies occurred over the East Asian middle latitudes and opposite anomalies occurred over the Ural Mountains and the Sea of Okhotsk at 500 hPa (Fig. 3g), accompanied by an enhancement and southward shift of the East Asian subtropical westerly jet (Fig. 3h). These
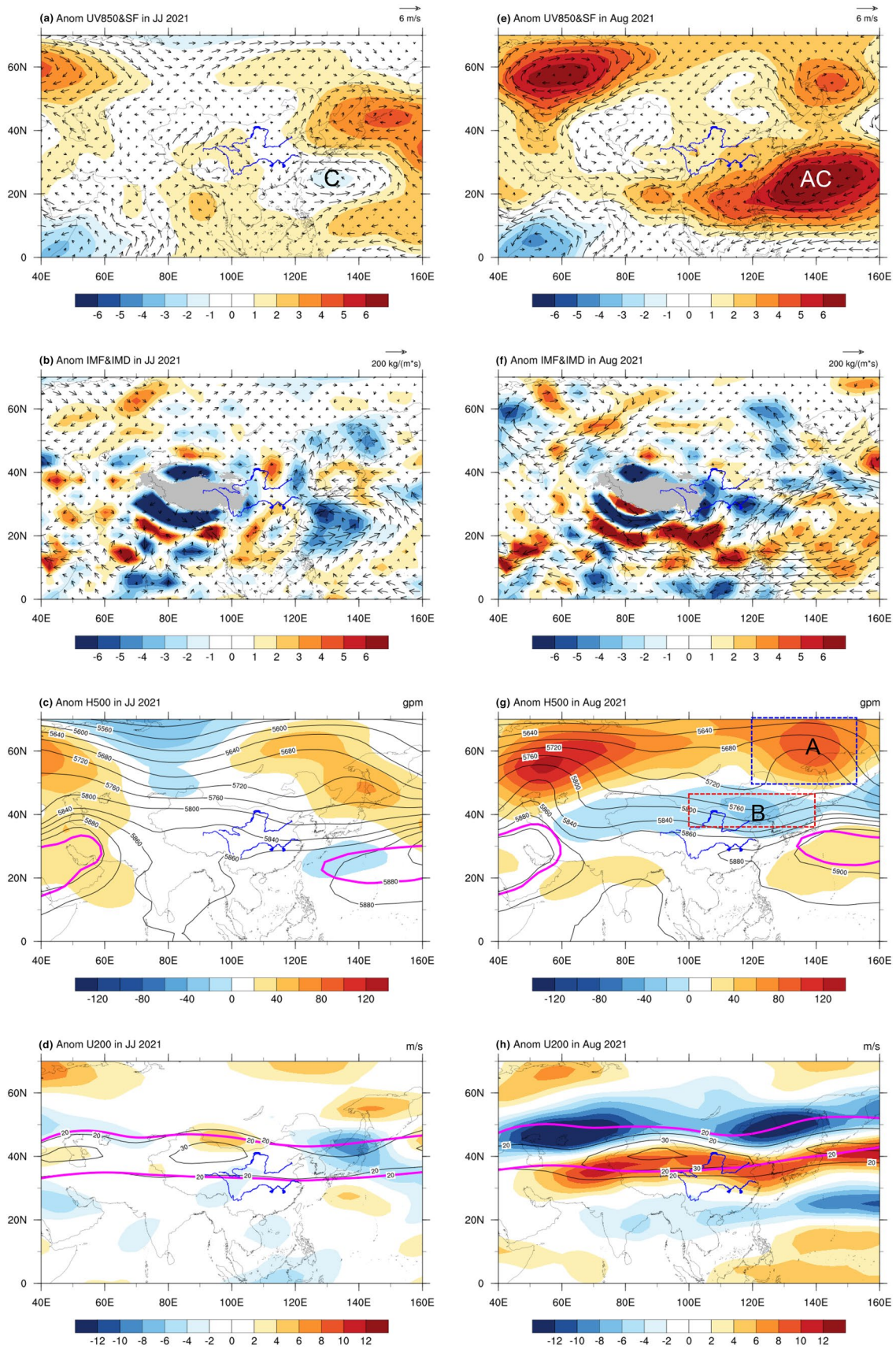
◄**Fig. 3** Atmospheric circulation patterns in **a–d** JJ and **e–h** August 2021: **a, e** 850-hPa horizontal wind (UV850; vectors; units: m s⁻¹) and stream function (SF; shadings; units: 10^5 m² s⁻¹) anomalies; **b, f** vertically integrated (surface to 300 mb) moisture flux anomalies (IMF; vectors; units: kg m⁻¹ s⁻¹) and moisture divergence anomalies (IMD; shadings; units: 10^{-5} kg m⁻¹ s⁻¹); **c, g** 500-hPa geopotential height (H500; contours; units: gpm) and anomalies (shadings), the pink contour indicates the climatological 5880 gpm; **d, h** 200-hPa zonal wind (U200; contours; units: m s⁻¹; starting from 20 with an interval of 10 m s⁻¹) and anomalies (shadings), the pink contour indicates the climatological mean. C and AC denotes cyclone and anticyclone, respectively. The East Asia cold air (EACA) index is defined as the difference in the H500 between the two boxes (the blue box minus the red box)

atmospheric circulation conditions favor the southward intrusion of middle–high latitude cold air into the YHRB region (Fig. 3e). In June–July 2021 (Fig. 3c, d), however, the atmospheric circulation anomalies over the Eurasian middle–high latitudes were obviously weaker than those in August. Moreover, the pattern of the circulation anomalies over East Asia in August 2021 was similar to that of the regressions against the YHRBPI during 1981–2020 (Fig. 3e–h vs. Supplementary Fig. 1e–h), supporting the important role of the East Asian middle–high latitude circulation anomalies on the precipitation anomalies over the YHRB region in August.

To represent the intensity of the East Asia cold air (EACA) in August, an EACA index was constructed as the difference in the 500-hPa geopotential height between Northeast Asia (50°–70° N, 120°–150° E) and East Asia middle latitudes (35°–45° N, 100°–140° E) (see the boxes in Fig. 3g), where the regressed H500 anomalies against the standardized YHRBPI are also significant and strong in August during 1981–2020 (Supplementary Fig. 1g). It is shown in Fig. 4b that the intensity of August EACA reached its historic peak in 2021. Moreover, more precipitation tends to occur over the YHRB region when the WNPAC and EACA indices are both strong in August (Fig. 5b). In particular, the extremely high index of the EACA and WNPAC coincided with the most extreme precipitation over the YHRB region in August 2021. In June–July, more precipitation generally occurred over the YHRB region when the WNPAC index was higher than one standard deviation (Fig. 5a), and the most extreme precipitation occurred in 2020, when the WNPAC was the strongest on record since 1981 (Fig. 4a).

To confirm the impact of subtropical and middle–high latitude atmospheric circulation anomalies on YHRB precipitation, the relationship of the YHRBPI with the WNPAC and EACA indices in June–July and August during 1981–2020 was further examined (see Supplementary Fig. 2). The WNPAC index is significantly correlated with the YHRBPI index, with a correlation coefficients of 0.55 ($p < 0.001$) and 0.48 ($p < 0.01$) in June–July and August, respectively. The

EACA index has correlations of 0.31 ($p < 0.05$) and 0.37 ($p < 0.05$) with the YHRBPI index in June–July and August, respectively. This result supports the combined effect of the subtropical and middle–high latitude circulation anomalies on the precipitation anomalies over the YHRB region.

To quantify the contribution of the WNPAC and EACA to the YHRB precipitation anomalies in 2021, the YHRBPI in August was reconstructed from the WNPAC and EACA indices in a multi-regression equation during 1981–2020 (see Supplementary Fig. 3). Notably, the correlation coefficient between the WNPAC and EACA is only 0.17 ($p > 0.10$) during 1981–2020, indicating that they are independent of each other. The WNPAC and EACA indices explain respectively 24.2% and 21.8% of the YHRBPI in August 2021, respectively, confirming their important contribution to the extreme YHRB precipitation event in 2021. It should be noted that there are still other circulation patterns linked to heavy precipitation in the YHRB region in some years, such as landfalling typhoons (Cheung et al. 2018), the eastward shortwave trough and the southwest vortex over the upstream region (Wang 1987; Wang and Gao 2003).

In addition, changes in the East Asian subtropical westerly jet (EASWJ) are also important to precipitation variability over East Asia during summer (Zhang et al. 2018). For example, the YHRBPI has a significant and out-of-phase relationship with the EASWJ position index ($R = -0.54$, $p < 0.001$) in August during 1981–2020 (Supplementary Table 1). The EASWJ in August 2021 almost reached its southernmost position since 1981 (Supplementary Fig. 5), consistent with the result obtained from the EACA index.

4 Tropical SST anomalies in 2021 and their possible influences

4.1 Observational analysis

Tropical SSTAs play an important role in driving the climate variability over the WNP–East Asian region during summer. The central–eastern TPO experienced a decaying La Niña event in spring and a developing La Niña-like state in late summer 2021 (Fig. 6a–d). From September 2020 to April 2021, the monthly Niño3.4 index was below -0.5 °C (Fig. 6e), and the southern oscillation index remained positive. According to Li et al. (2022), there was a strong La Niña event starting in August 2020 and ending in April 2021, with a center located near the eastern TPO (the Niño3 region; Fig. 6a). The cold SSTAs in the central–eastern TPO were weaker in June–July (Fig. 6c) than those in spring (Fig. 6b), and became colder beginning in August (Fig. 6d). Results from real-time monitoring show that the SST cooling in the eastern TPO is developing into another

Fig. 4 Time series of the normalized **a** WNPAC and **b** EACA indices in June–July (blue) and August (red) during 1981–2021
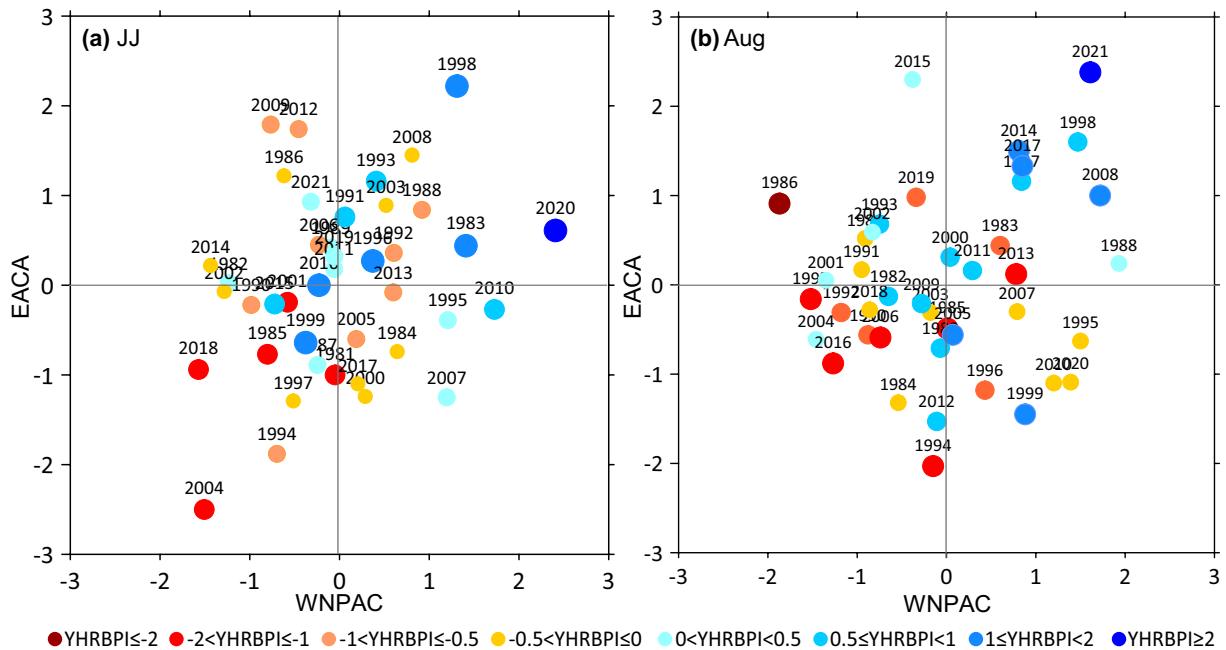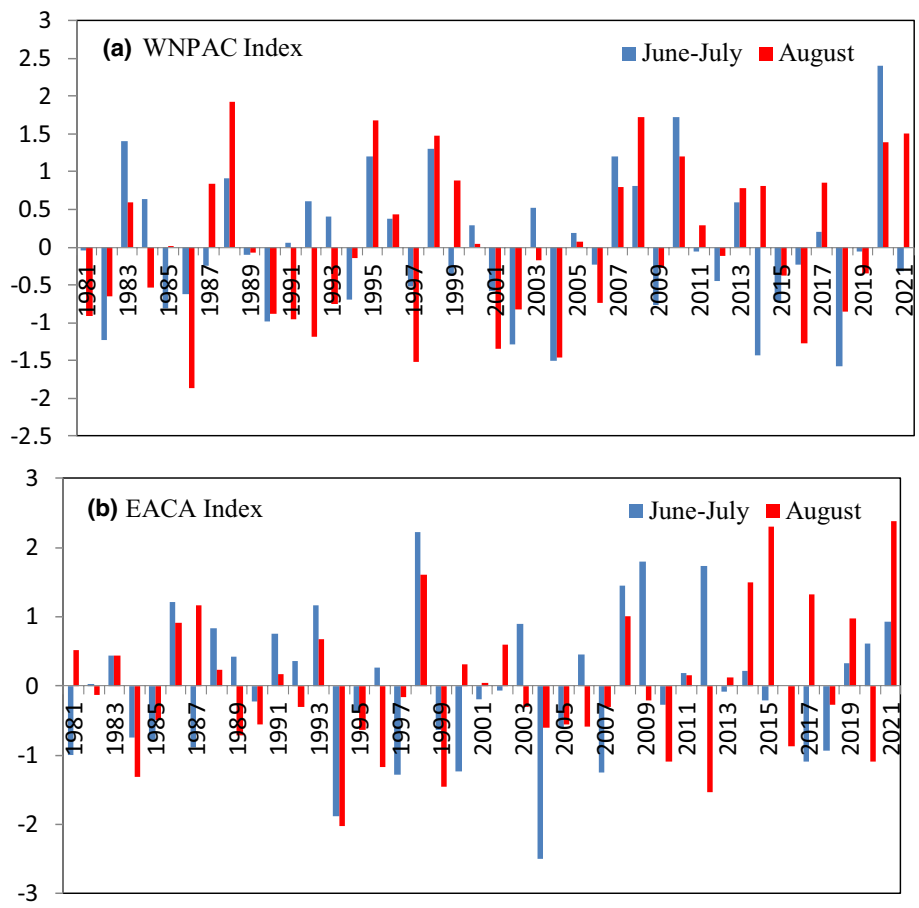

Fig. 5 Scatterplots of the EACA index versus the WNPAC index in **a** JJ and **b** August during 1981–2021. Shaded dots indicate the amplitude of the YHRBPI
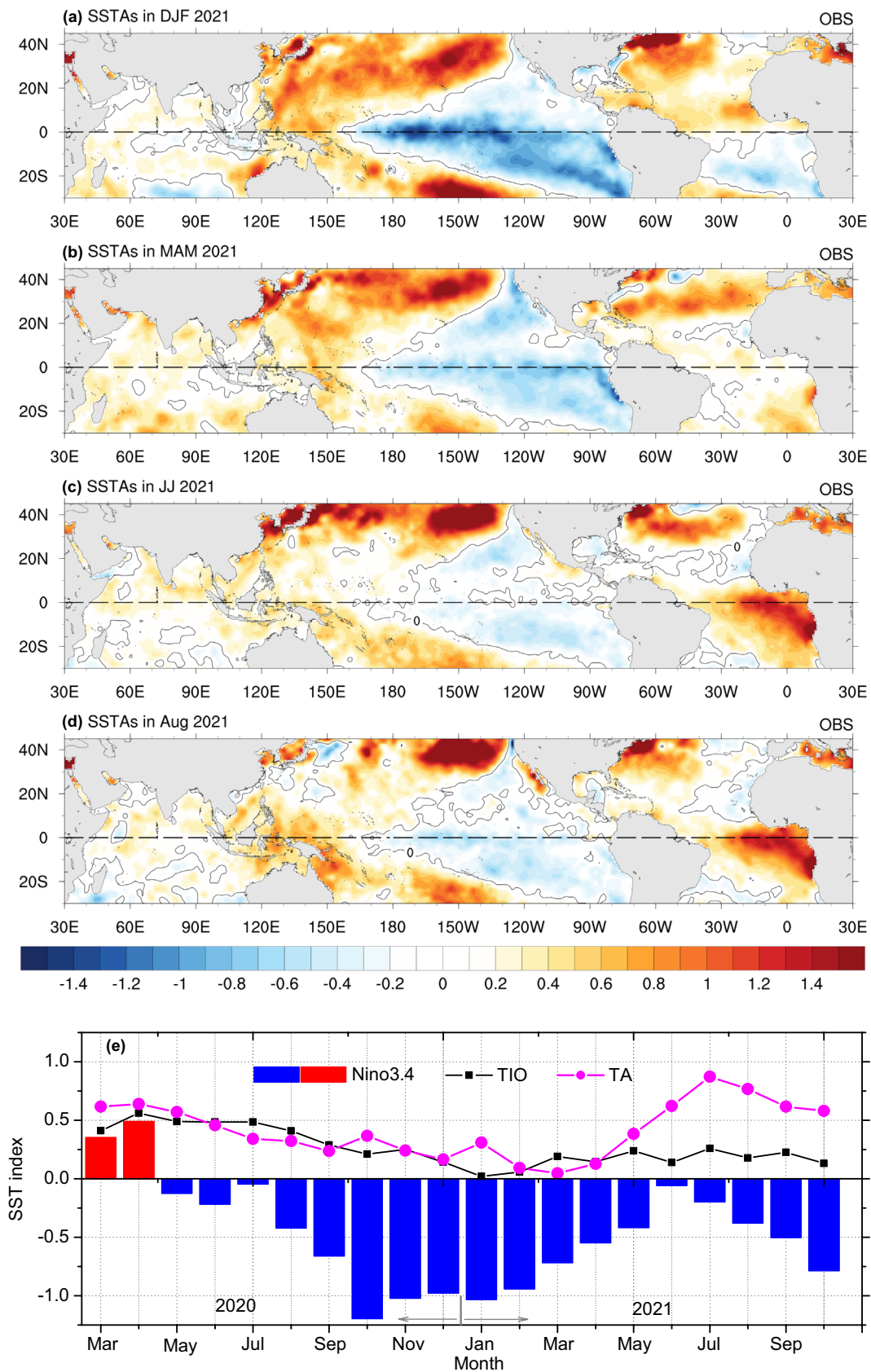
Fig. 6 SST anomalies (units: °C) in **a** DJF, **b** MAM, **c** JJ, and **d** August 2021. **e** Time series of the Niño 3.4 index, TIO index and TA index (units: °C) from March 2020 to October 2021

La Niña event in the subsequent autumn and winter, which is agrees the previous results that La Niña events can occur after another La Niña (Hu et al. 2014).

Consistent with the cold SSTAs in the central–eastern TPO associated with the La Niña event, there was a persistent anomalous cyclone around the Philippine Sea in the lower troposphere and below-normal precipitation in southern China from winter 2020 to early summer 2021 (Liu and Gao 2021; Zhao et al. 2022a). This is consistent with previous studies showing that an anomalous low-level cyclone is likely to generate around the Philippine Sea following a La Niña event (Wang et al. 2000; Tao et al. 2017; Feng et al. 2017), leading to light precipitation in the YHRB region (Wu et al. 2010). However, the strong WNPAC and thus heavy precipitation anomalies in the YHRB region in August 2021 occurred under the La Niña decaying state, implying that other factors may contribute to the extreme case in 2021.

The TIO showed persistent warming from March to August 2021, with a value of the TIO index between 0.14 and 0.26 °C (Fig. 6e), less than one standard deviation (between 0.24 and 0.29 °C). This indicates that the TIO warming was relatively weak in spring and summer 2021. In contrast to the TIO warming, the overlying convection activity was suppressed (i.e., positive OLR and negative precipitation anomalies) over the eastern TIO in June–July (Fig. 7a, b). In August, the strong negative OLR and positive precipitation anomalies over the eastern TIO (Fig. 7e, f) were primarily related to the active MJO activity, which will be discussed in later section. These results suggest that weak TIO warming could not explain the obvious subseasonal variation in the WNPAC in August 2021.

Notably, the warm SSTAs over the tropical Atlantic enhanced rapidly from spring to summer 2021, with the value of the TA index increasing from 0.05 °C in March to 0.87 °C in July (Fig. 6e). The TA index was 0.38 °C and 0.62 °C in May and June 2021, respectively, both of which were higher than one times their standard deviations (0.29 °C and 0.38 °C, respectively). The TA index was 0.87 °C and 0.77 °C in July and August 2021, respectively, which were higher than two times of their standard deviations (0.35 °C and 0.33 °C, respectively). In June–July, the OLR (precipitation) anomalies are positive (negative) over the TA (Fig. 7a,
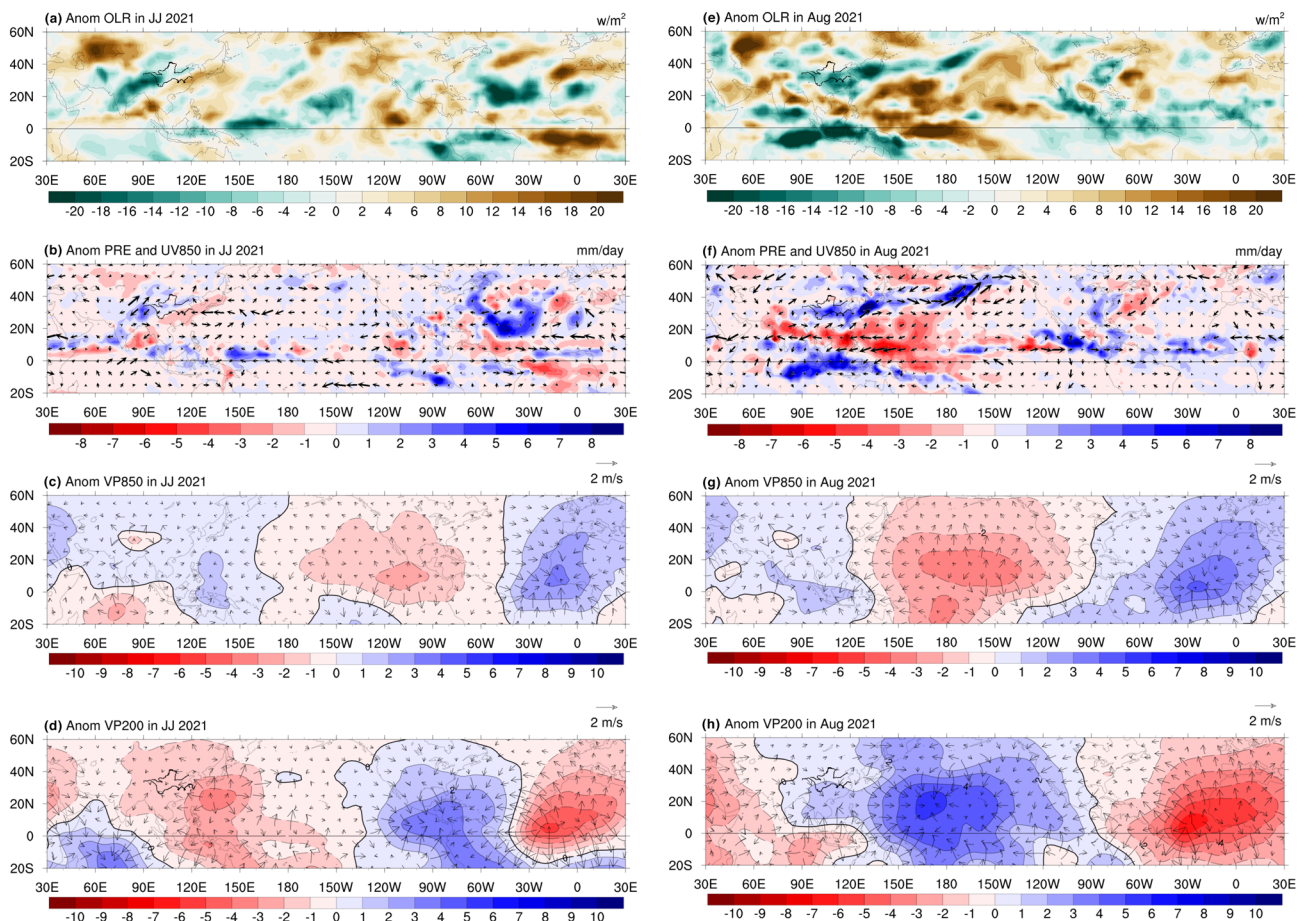

Fig. 7 Anomalies of **a** OLR, **b** precipitation (units: mm/day) and horizontal wind (vector; units: m s^{-1}) at 850-hPa, velocity potential (shading, units: 10^6 m^2 s^{-1}) and divergent wind (vector, units: m s^{-1}) at **c** 850-hPa and **d** 200-hPa in JJ 2021. **e–h** are same as **a–d**, but for August 2021

b). In August, opposite OLR and precipitation anomalies are observed over the TA (Fig. 7e, f), accompanied by anomalous low-level convergence and upper-level divergence in that region (Fig. 7g, h). This suggests that the warm SSTAs in the TA favored strong local convection activity, and might contribute to the enhancement of the WNPAC and thus the heavy YHRB precipitation anomalies in August 2021 (Hong et al. 2014, 2015; Zuo et al. 2019). In addition, the WNPAC index in August is significantly correlated with the TA, Niño3.4 and TIO index in July–August, with a correlation coefficients of 0.59 ($p < 0.001$), − 0.48 ($p < 0.01$) and 0.36 ($p < 0.05$) during 1981–2020, respectively (see Supplementary Fig. 6 and Supplementary Table 2). This indicates that the WNPAC in August is more closely related to the SSTAs in the TA and the TPO than that in the TIO.

4.2 Numerical experiments

We designed a series of numerical experiments to validate the influences of tropical SSTAs on the large-scale atmospheric circulation and thus the YHRB precipitation anomalies in August 2021. The global climatological SST with an annual cycle drives the CAM5.3 model in the control (CTL) run. Considering the SSTA intensity and persistence in 2021, the sensitivity runs were forced by the observed SSTAs in May–August 2021 over the TA, TPO, and their combinations (Table 1). These experiments are referred to as TA2021, TPO2021 and TA+TPO2021 experiments, respectively. Atmospheric circulation responses to SSTAs forcing are defined as the difference in the ensemble–mean between the sensitivity experiments and the control run.

Figure 8 presents the responses of the stream function, horizontal wind and velocity potential anomalies in the TA2021 experiment. In June–July, an anomalous cyclonic response occurs over the subtropical eastern Pacific–North Atlantic and an anomalous anticyclonic response occurs over the WNP at 850 hPa (Fig. 8a). However, the amplitudes of the responses are relatively weak. Similar patterns of the responses are observed in August, but with amplitudes much stronger than those in June–July. In addition, there are evidently positive precipitation responses over the TA in August (figures not shown), and the associated diabatic heating triggers a pair of Gill-type low-level cyclonic responses over the subtropical eastern Pacific–western Atlantic (Fig. 8d), which are similar to their observed counterparts (Fig. 7f). Furthermore, there are anomalous low-level convergence and upper-level divergence responses over the TA and opposite responses over the central tropical Pacific in August (Fig. 8e, f), with an amplitude obviously stronger than that in June–July. These results reveal that the TA warming benefits enhanced subsidence and thus weakened convection activity over the central tropical Pacific, which further enhances the
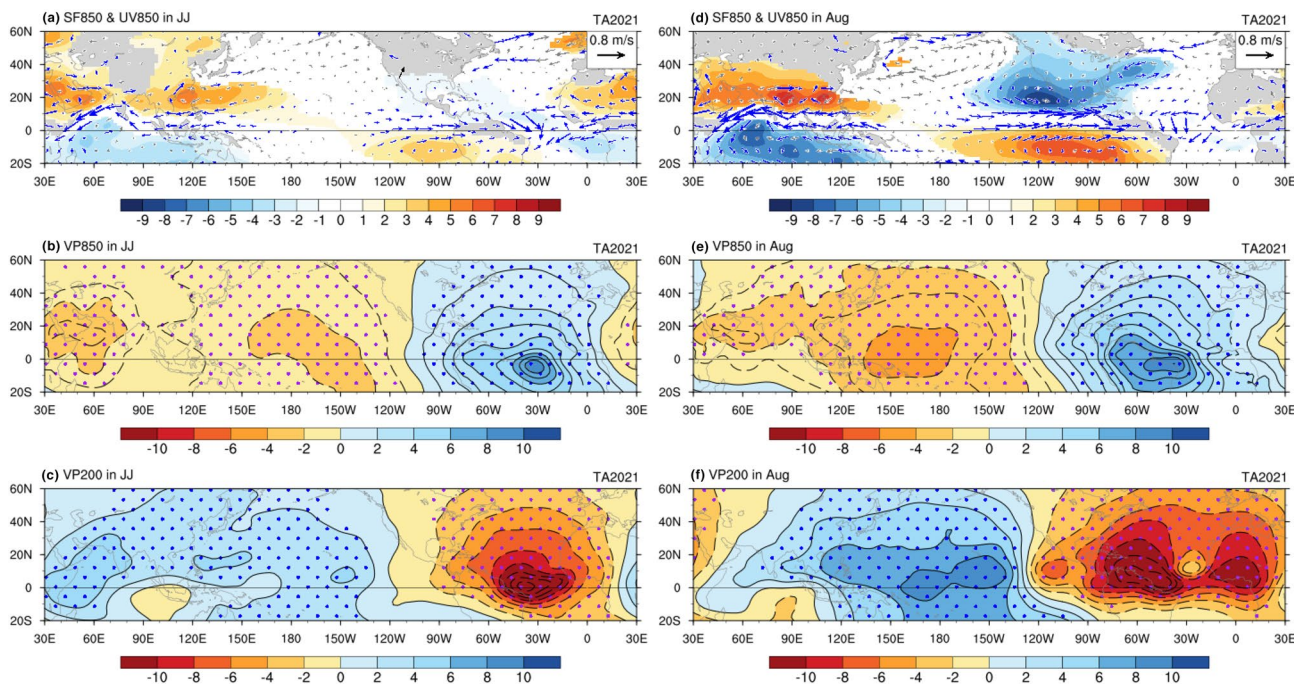

Fig. 8 a Anomalies of horizontal wind (vectors; units: m s^{-1}) and stream function (shadings; units: 10^5 m^2 s^{-1}) at 850-hPa, velocity potential anomalies (units: 10^6 m^2 s^{-1}) at **b** 850 hPa and **c** 200-hPa averaged during June–July in response to the anomalous TA SST forcing in 2021. Blue vectors in **a** and dots in **b**, **c** represent significance at 95% confidence level. **d–f** are the same as **a–c**, but for August

WNPAC by triggering a Gill-type Rossby-wave response to the west of the subsidence in August (Gill 1980). This result agrees with previous studies showing that warm SSTAs in the TA favor the strengthening of the WNPAC by modulating the Walker circulation over the Atlantic–Pacific Oceans during boreal summer (Hong et al. 2014; Chang et al. 2016; Zuo et al. 2019; Zhao et al. 2021, 2022b). Therefore, subseasonal changes in the WNPAC response to the TA SST forcing in the sensitivity experiments are consistent with their observed counterparts, confirming that rapid TA warming had an important contribution to the subseasonal change in the WNPAC and thus extreme precipitation over the YHRB during summer 2021.

Notably, the TA warming peaked in July 2021, whereas the WNPAC response became much stronger in the following August. This is consistent with previous studies showing that the responses of tropical atmospheric circulation tend to lag the TA SST forcing by approximately one month during summer (Jin and Hoskins 1995; Zuo et al. 2019). Moreover, the WNP monsoon trough moves further northward in August than in June–July (Xiang et al. 2013), which provides a favorable background for a stronger WNPAC response to the TA SST forcing in August (Zuo et al. 2020). Finally, cold SSTAs in the central–eastern TPO associated with the second La Niña event developing in summer could also provide favorable conditions for the enhancement of the TA-induced anomalous overturning Walker circulation over the Pacific–Atlantic Oceans. As shown in Fig. 9, there are low-level easterly wind responses in the tropical western

Pacific and divergence responses over the central tropical Pacific in both June–July and August in the TPO2021 experiment, which are consistent with the Matsuno–Gill theory (Gill 1980). In addition, a low-level anti-cyclonic response is observed in August in the TPO2021 experiments (Fig. 9d), indicating that the cold SSTAs in the central–eastern tropical Pacific associated with the second La Niña event also contributed to the enhancement of the WNPAC in August 2021.

To validate the combined effect of the TPO and TA SSTAs, Fig. 10 shows the atmospheric circulation response in the TA+TPO2021 experiments. A comparison of Figs. 10 and 8 indicates that the pattern of the tropical atmospheric circulation responses in the TA+TPO2021 experiment resembles that in the TA2021 experiment. This implies that the atmospheric circulation response in the tropics was primarily dominated by the TA SSTAs, which is consistent with the fact that SST anomalies in the TPO were relatively weak in 2021 when compared to those in the TA.

Moreover, probability distribution functions (PDFs) of the simulated YHRBPI and WNPAC in August for the different experiments were further examined (Fig. 11). It is indicated that the WNPAC index clearly shifts to its high index phase in all the sensitivity experiments when compared to the control run in August (Fig. 11b), with a shift more obvious in the TA2021 and TA+TPO2021 experiments. This is consistent with the aforementioned result that both the TA and TPO SSTAs contributed to the strong WNPAC in August 2021 and that the TA SSTAs played a more important role. Consistently, the precipitation response
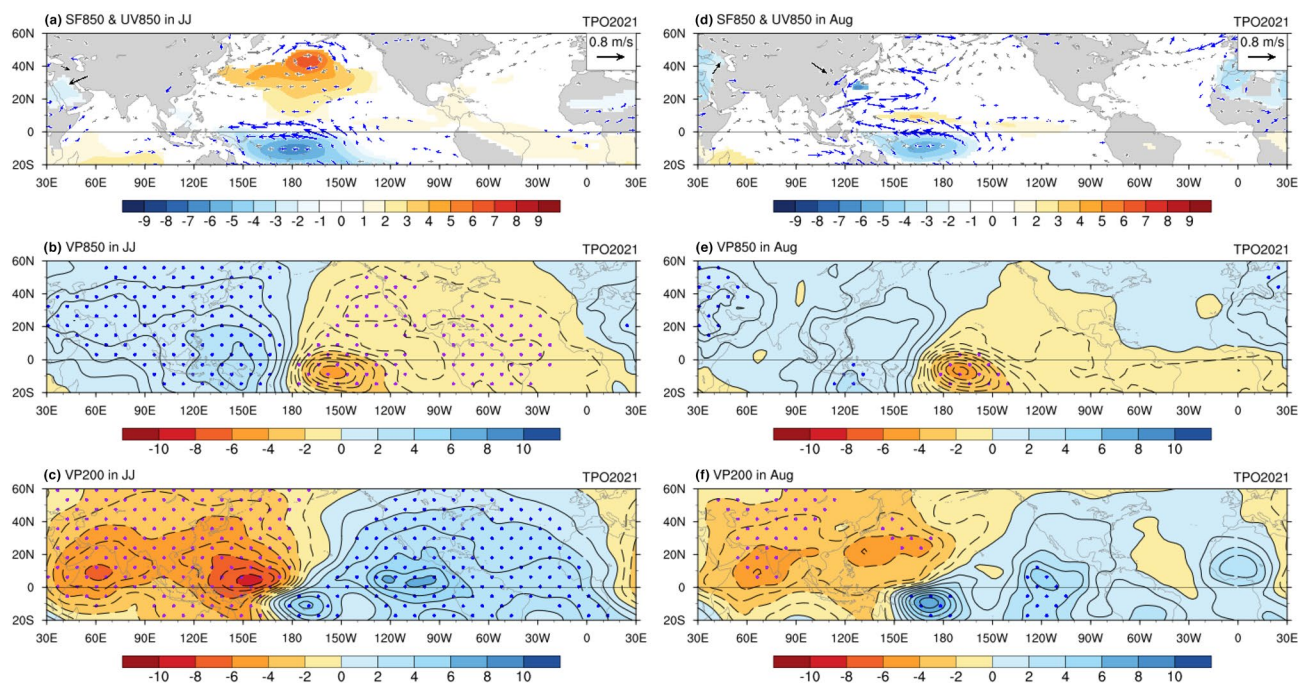

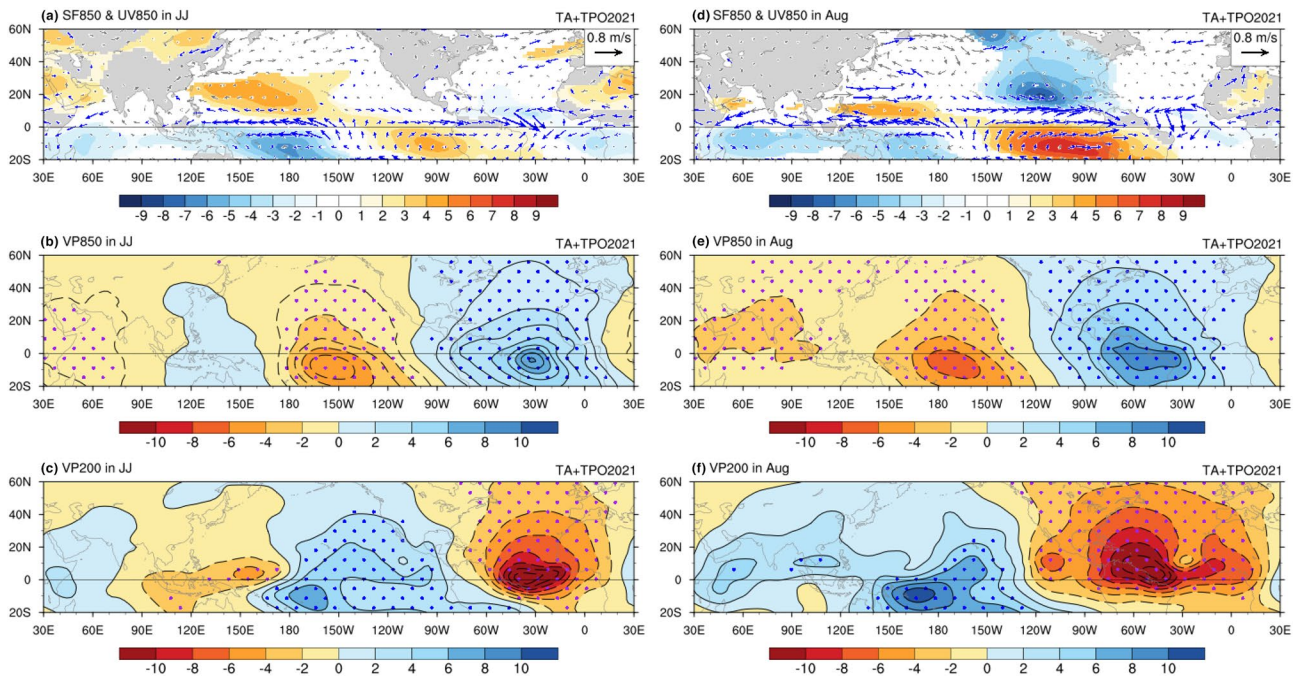**Fig. 9** Same as Fig. 8, but for the TPO2021 experiment

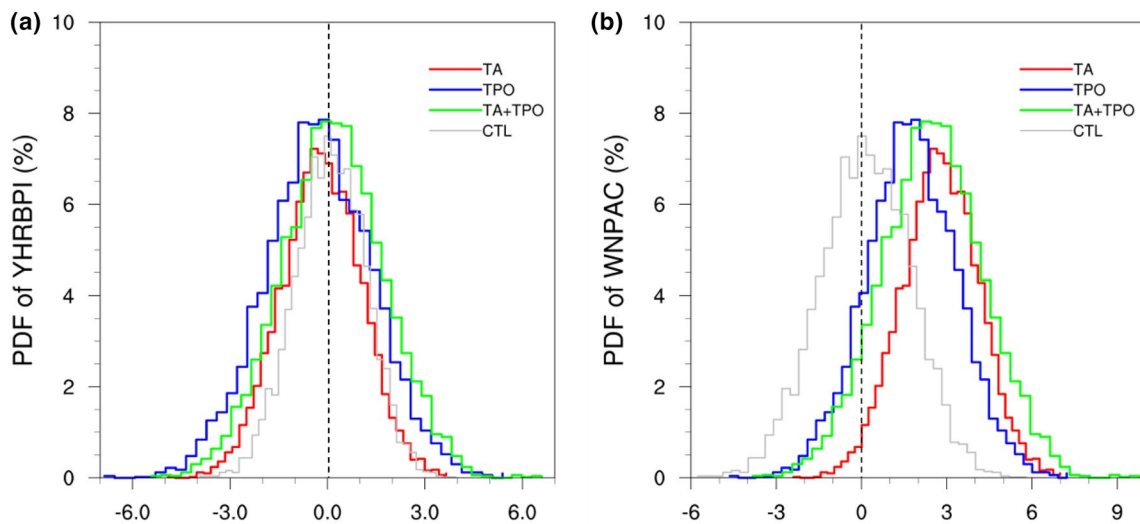**Fig. 10** Same as Fig. 8, but for the TA + TPO2021 experiment

Fig. 11 Probability distribution functions (PDFs) of the **a** YHRBPI and **b** WNPAC in August in the control run (grey line) and sensitivity experiments

over the YHRB region is stronger in the TA + TPO2021 experiment, and the occurrence of extreme precipitation events is more frequent in both the TPO and TA + TPO2021 experiments than in the control run (Fig. 11a). Although the warmer TA SSTAs benefit a strong WNPAC, the probability of above-normal YHRB precipitation anomalies increases moderately. This may be related to the southward shift of the WNPAC in the experiment compared with that in the

observation, and the distribution of precipitation anomalies is sensitive to the location and shape of the WNPAC. Nevertheless, the large-scale atmospheric circulation (i.e., the WNPAC) response is robust in the sensitivity experiments, and the precipitation response is generally consistent with the large-scale atmospheric circulation response, especially in the combined sensitivity experiment.
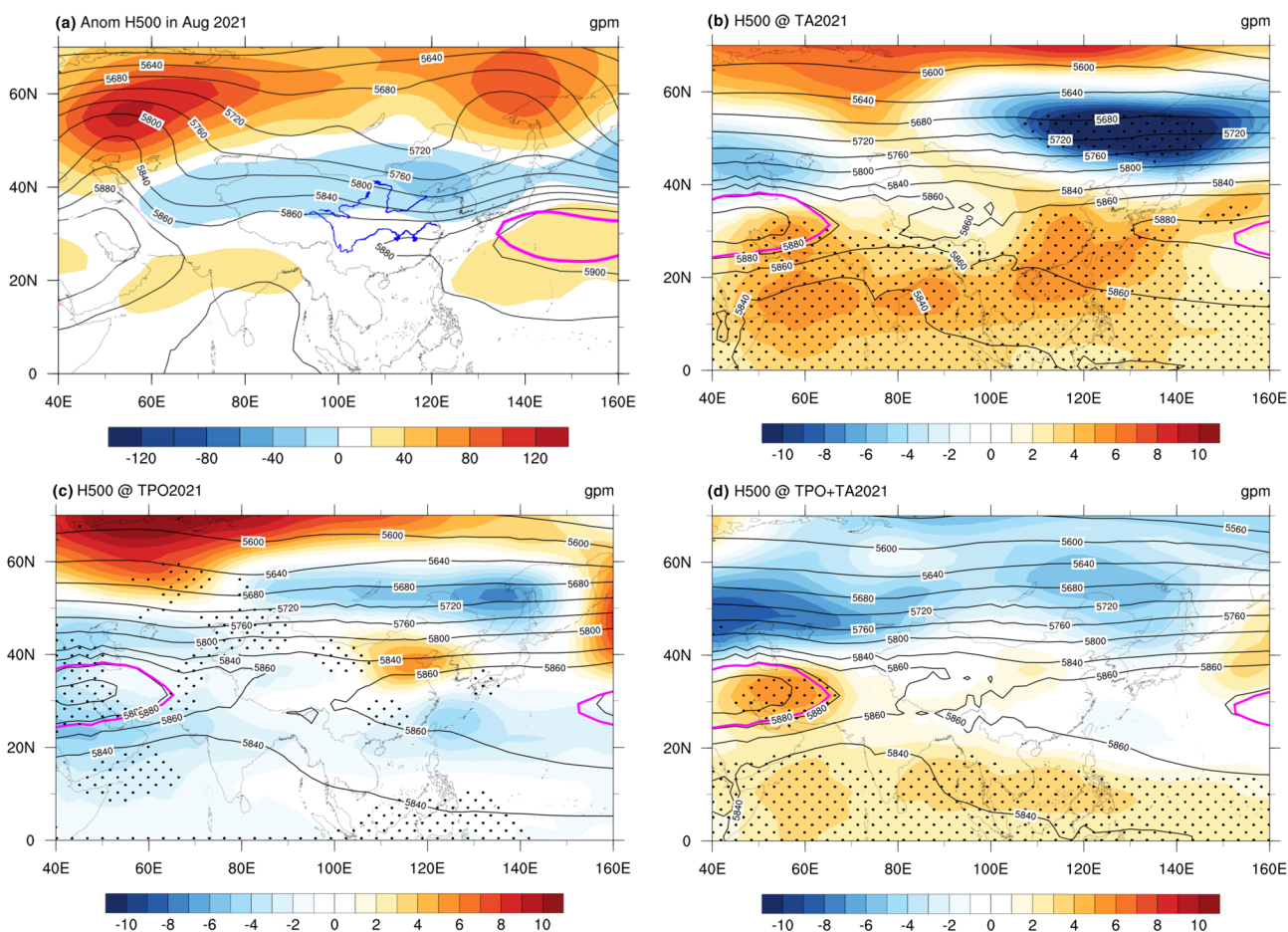
Fig. 12 H500 (black contour; units: gpm) and their anomalies (shading; units: gpm) in August 2021 derived from the **a** observation, **b** TA2021, **c** TPO2021 and **d** TA+TPO2021 experiments. Pink contour indicates the climatological mean of the H500 (unit: gpm) with a value of 5880 in the observation and the control run. Dots represent significance at the 95% confidence level

We have shown that the atmospheric circulation anomalies over the East Asian middle–high latitudes were very important to the precipitation anomalies over the YHRB region in August 2021 (Fig. 5b). However, the middle–high latitude circulation responses in all the sensitivity experiments are obviously different from their observed counterparts in August 2021 (Fig. 12), although the model can reasonably reproduce the observed circulation anomalies over the tropics and subtropics. For instance, the 500-hPa geopotential height response is negative over the Sea of Okhotsk in the TA2021 and TPO2021 experiments, which is opposite to the observed response. This implies that the relatively weak precipitation response over the YHRB is possibly related to the failure of the model in reproducing the large-scale atmospheric circulation anomalies over the East Asian mid–high latitudes. To confirm this notion, we divided the model outputs into two categories based on the above- and below- normal precipitation responses over the YHRB in August and then examined the behavior of the WNPAC and EACA in each group (Supplementary Fig. 7).

In the group with an above-normal precipitation response, the average value and minimum value of both the WNAPC and EACA are higher than those in the group with a below-normal precipitation response in all the sensitivity experiments. Moreover, the ensemble-mean WNPAC response is positive in both groups, while the EACA response tends to be positive (negative) in the group with an above- (below-) normal precipitation response. Therefore, this result confirms the robustness of the WNPAC response, and the relatively weak EACA response likely contributed to the weak YHRB precipitation response in the sensitivity experiments.

5 Conclusions and discussion

During the Meiyu period in June–July 2021, the YHRB region experienced normal precipitation. In August, the YHRB suffered reoccurrence of Meiyu and devastating precipitation extremes, and the regionally averaged precipitation amount listed the highest value since 1981, resulting

in severe floods and disasters. Such a remarkable subseasonal change in the YHRB precipitation anomalies was closely related to the subseasonal change in the WNPAC and East Asian middle–high latitude atmospheric circulation anomalies in summer 2021, which played an important role in controlling moisture transport and cold air activity that converge over the YHRB region, respectively. This study reveals the mechanism of the subseasonal change in the summer WNPAC and thus YHRB precipitation anomalies in 2021 through observational diagnosis and numerical model experiments.

The results showed that the rapid tropical Atlantic warming from late spring to summer and the second La Niña-like event in late summer contributed to the strong WNPAC and thus extreme precipitation over the YHRB in August 2021. There was a strong eastern-Pacific La Niña that rapidly decayed in spring and developed into another La Niña event in August 2021, accompanied by weak SSTAs in the TIO. Such a decaying La Niña event and the weak TIO SSTAs alone seem to be insufficient to induce the strong WNPAC in August 2021, since anomalous cyclonic flows are likely to be generated around the Philippine Sea following a La Niña event. In contrast, warm SSTAs in the TA rapidly strengthened from May to June, and persisted until August, which observably contributed to the enhancement and westward shift of the WNPAC by inducing a westward-extending overturning circulation over the Pacific–Atlantic Oceans in August 2021. Moreover, the cold SSTAs in the eastern tropical Pacific associated with the second La Niña event provided favorable conditions for a strong WNPAC in August. Notably, the 2020/2021 La Niña event was followed by another La Niña that emerged in August 2021, and whether the previous event has an impact on the development of the follow-up event and thus the WNPAC remains unclear, and deserves further study in future works.

Finally, we found that the MJO was active and long-lasting over the tropical Indian Ocean in August 2021 (Zhao et al. 2022a), which is obviously different from the eastward propagation characteristics of classical MJO events. Convection activity associated with MJO activity has been recognized as a vital factor contributing to extreme precipitation anomalies over East Asia (Hsu et al. 2020; Zhang et al. 2021). The MJO activity in August 2021 was obviously different from that in June–July 2021 (Fig. 13a); that is, the MJO activity was weak in early June and active over the western hemisphere in late June, while in July, the MJO activity moved eastward from the western TIO into the western Pacific. In contrast, during August 2021, the MJO was persistently active over the western Indian Ocean for 26 days, far beyond its climatology (Fig. 13b). Wang et al. (2019a) classified this kind of MJO activity as a "standing" type. To investigate the possible impact of the standing type of MJO event on East Asian climate variability, we display in Fig. 13c the composite
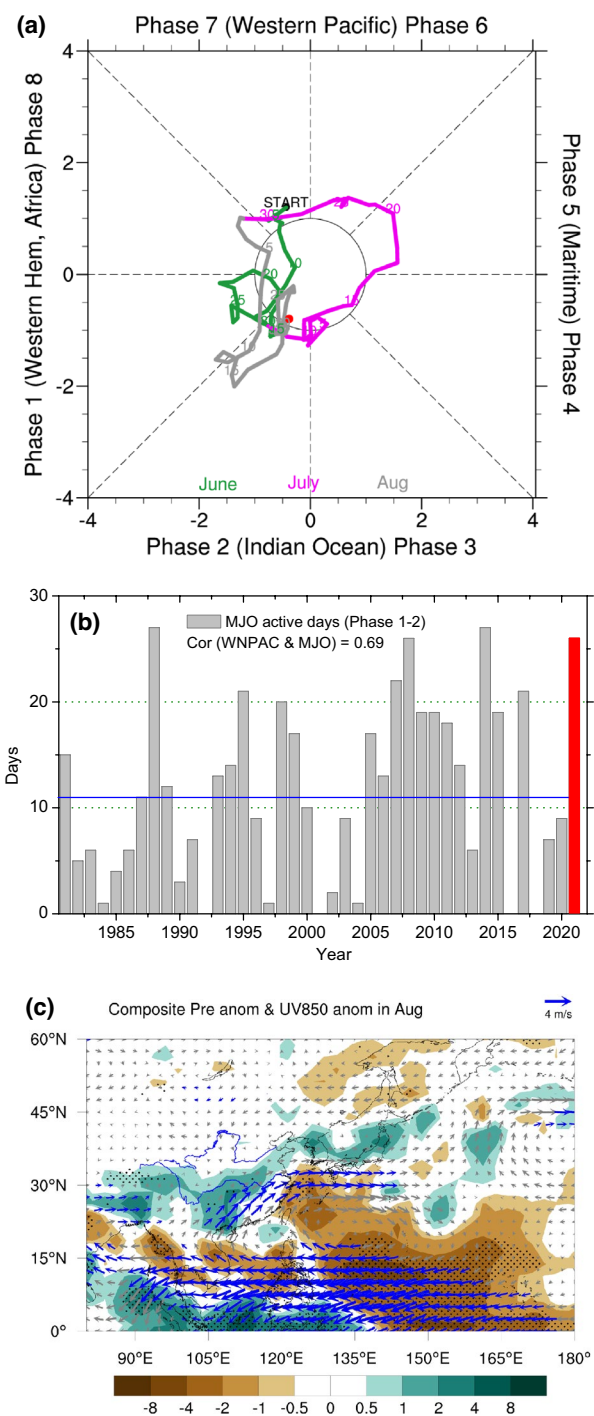

Fig. 13 a The phase space diagram of MJO active from June 1 to August 31, 2021, with green, pink and gray for the June, July and August, respectively. **b** Time series of the August MJO active days in Phases 1–2 from 1981 to 2021. The red bar denotes the year 2021. **c** Composite precipitation (shading; unit: mm/day) and wind anomalies at 850-hPa (vectors; units: m/s) for the MJO active years in Phases 1–2 in August during 1981–2020. Dots and blue vectors indicate significant at 95% confidence level
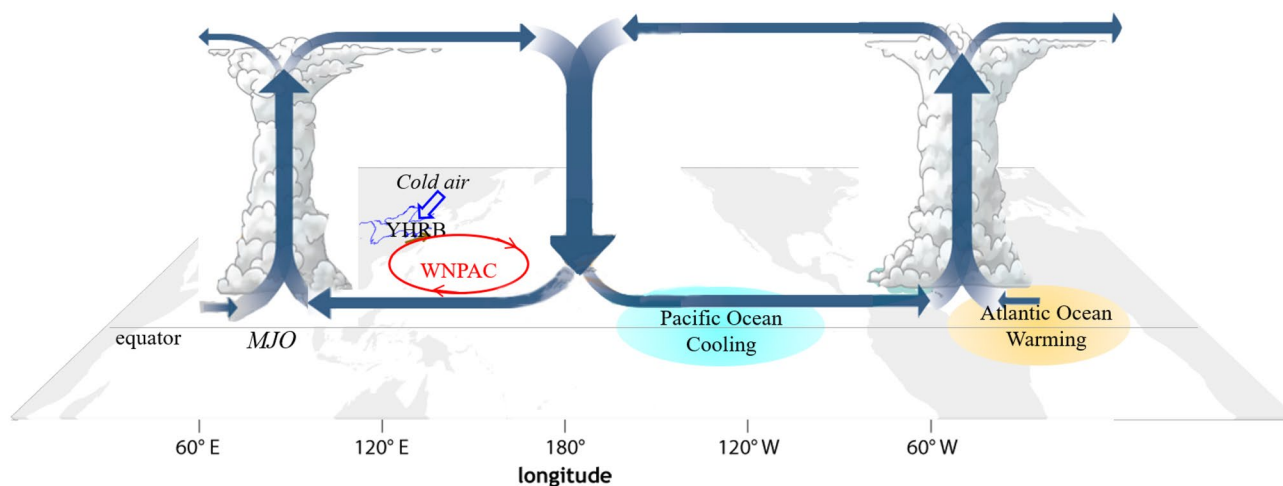
Fig. 14 Schematic diagram explaining what drives the extreme precipitation over the YHRB in August 2021

anomalies of the horizontal wind at 850 hPa and precipitation with respect to Phases 1–2 of the MJO events with more than 20 active days in August during 1981–2020. Corresponding to the enhanced convection activity in the western TIO for MJO Phases 1–2, a strong anomalous anticyclone and suppressed convection activity dominate the WNP, which benefits abundant water vapor from the Indo-Pacific Oceans to East Asia (Fig. 13b). Similar anomalies of convection and atmospheric circulation occurred in August 2021 (Fig. 7f). This indicates that the MJO persisting in Phases 1–2 may play an anchoring role in maintaining the strengthening of the WNPAC in August 2021. However, the cause of the anomalous MJO activity in August remains unclear.

Figure 14 shows a schematic diagram explaining the main drivers of the robust WNPAC and heavy precipitation over the YHRB in August 2021. We emphasize the important role of the rapid warming of tropical Atlantic SSTAs and the second developing La Niña event, particularly the lagged effects of the former. Moreover, in this paper, we focused on SSTAs forcing to find the pre-signal for climate prediction. It should be noted that MJO activity is another important factor worth investigating. In addition, atmospheric circulation anomalies over the East Asian middle–high latitudes are very important to the YHRB precipitation anomalies in August. However, the maintenance mechanism of the record-breaking middle–high latitude circulation anomalies in August 2021 remains unclear. The seasonal evolution of tropical SSTAs in 2021 is obviously different from that associated with the EACA index in August (Fig. 6 vs Supplementary Fig. 8), and the SSTAs are even opposite in sign in the equatorial central–eastern Pacific, implying that the EACA extreme in August 2021 was likely related to other factors instead of

the tropical SSTAs emphasized in this study. The observed atmospheric circulation anomalies over the mid–high latitudes in August 2021 might be related to interval variability and/or other underlying boundary forcings, such as the spring Arctic sea ice concentration, Eurasian snow cover and soil moisture (Wu et al. 2009; Zhang and Zuo 2011; Zhang et al. 2017), which needs further examination in future works.

Data availability statement The GPCP precipitation data can be accessed from https://psl.noaa.gov/data/gridded/data.gpcp.html. The NCEP-NCAR atmospheric circulation reanalysis data are taken from http://www.esrl.noaa.gov/psd/data/gridded/data.ncep.reanalysis.derived.html. The OLR data are available at https://www.ncei.noaa.gov/products/climate-data-records. The HadISST data are from https://www.metoffice.gov.uk/hadobs/. The observed daily precipitation data are provided by the National Meteorological Information Center of China Meteorological Administration and available from the corresponding author upon reasonable request.

Declarations

Conflict of interest The authors declare no conflict of interest.

References

Adler R, Sapiano Mathew RP, Huffman GJ et al (2018) The global precipitation climatology project (GPCP) monthly analysis (new version 2.3) and a review of 2017 global precipitation. Atmosphere 9:138. https://doi.org/10.3390/atmos9040138

Chang TC, Hsu HH, Hong CC (2016) Enhanced influences of tropical Atlantic SST on WNP–NIO atmosphere–ocean coupling sincethe early 1980s. J Clim 29:6509–6525. https://doi.org/10.1175/JCLI-D-15-0807.1

Chang CP, Zhang YS, Li T (2000) Interannual and interdecadal variations of the East Asian summer monsoon and tropical Pacific SSTs. Part I: roles of the subtropical ridge. J Clim 13:4310–4325. https://doi.org/10.1175/1520-0442(2000)0132.0.CO;2

Chen W, Park J-K, Dong BW et al (2012) The relationship between El Niño and the western North Pacific summer climate in a coupled GCM: role of the transition of El Niño decaying phases. J Geophys Res 117:D12111. https://doi.org/10.1029/2011JD017385

Cheung HM, Ho CH, Jhun JG et al (2018) Tropical cyclone signals on rainfall distribution during strong vs. weak Changma/Baiu years. Clim Dyn 51:2311–2320. https://doi.org/10.1007/s00382-017-4014-1

Ding YH (1992) Summer monsoon rainfalls in China. J Meteorol Soc Jpn 70:373–396. https://doi.org/10.2151/jmsj1965.70.1B_373

Ding YH, Liang P, Liu YY et al (2020) Multiscale variability of Meiyu and its prediction: a new review. J Geophys Res Atmos 125:e2019JD031496. https://doi.org/10.1029/2019JD031496

Ding YH, Liu YY, Hu ZZ (2021) The record-breaking Meiyu in 2020 and associated atmospheric circulation and tropical SST anomalies. Adv Atmos Sci 38:1980–1993. https://doi.org/10.1007/s00376-021-0361-2

Feng J, Chen W, Li YJ (2017) Asymmetry of the winter extra-tropical teleconnections in the Northern Hemisphere associated with two types of ENSO. Clim Dyn 48:2135–2151. https://doi.org/10.1007/s00382-016-3196-2

Gill AE (1980) Some simple solutions for the heat induced tropical circulation. Q J Meterol Soc 106:447–462. https://doi.org/10.1002/qj.49710644905

He JH, Wu ZW, Jiang Z et al (2007) "Climate effect" of the northeast cold vortex and its influences on Meiyu. Sci Bull 51:671–679. https://doi.org/10.1007/s11434-007-0053-z

Hong C-C, Chang T-C, Hsu H-H (2014) Enhanced relationship between the tropical Atlantic SST and the summertime western North Pacific subtropical high after the early 1980s. J Geophys Res Atmos 119:3715–3732. https://doi.org/10.1002/2013JD021394

Hong C-C, Lee M-Y, Hsu H-H et al (2015) Tropical SST forcing on the anomalous WNP subtropical high during July–August 2010 and the record-high SST in the tropical Atlantic. Clim Dyn 45:633–650. https://doi.org/10.1007/s00382-014-2275-5

Hsu P-C, Qian Y, Liu Y et al (2020) Role of abnormally enhanced MJO over the Western Pacific in the formation and subseasonal predictability of the record-breaking Northeast Asian heatwave in the summer of 2018. J Clim 33:3333–3349. https://doi.org/10.1175/JCLI-D-19-0337.1

Hu ZZ, Kumar A, Xue Y et al (2014) Why were some La Niñas followed by another La Niña? Clim Dyn 42:1029–1042. https://doi.org/10.1007/s00382-013-1917-3

Hurrell JW, Holland MM, Gent PR et al (2013) The community earth system model: a framework for collaborative research. Bull Am Meteorol Soc 94:1339–1360. https://doi.org/10.1175/BAMS-D-12-00121.1

Jin FF, Hoskins BJ (1995) The direct response to tropical heating in a baroclinic atmosphere. J Atmos Sci 52:307–319

Kalnay E, Kanamitsu M, Kistler R et al (1996) The NCEP/NCAR 40-year reanalysis project. Bull Am Meteorol Soc 77:437–471. https://doi.org/10.1175/1520-0477(1996)077%3c0437:tnyrp%3e2.0.co;2

Kang IS, Jin K, Wang B et al (2002) Intercomparison of the climatological variations of Asian summer monsoon precipitation simulated by 10 GCMs. Clim Dyn 19:383–395. https://doi.org/10.1007/s00382-002-0245-9

Li WJ (1999) General atmospheric circulation anomaly in 1998 and their impact on climate anomaly in China. Meteorol Mon 25:20–25. https://doi.org/10.3969/j.issn.1000-0526.1999.04.004. ((in Chinese))

Li T, Wang B (2005) A review on the western North Pacific monsoon: synoptic-to-interannual variabilities. Terr Atmos Ocean Sci 16:285–314. https://doi.org/10.3319/TAO.2005.16.2.285(A)

Li Y, Lu R, Dong B (2007) The ENSO-Asian monsoon interaction in a coupled ocean-atmosphere GCM. J Clim 20:5164–5177. https://doi.org/10.1175/JCLI4289.1

Li T, Wang B, Wu B et al (2017) Theories on formation of an anomalous anticyclone in western North Pacific during El Niño: a review. J Meteorol Res 31:987–1006. https://doi.org/10.1007/s13351-017-7147-6

Li WJ, Ren HC, Zuo JQ, Ren HL (2018) Early summer southern China rainfall variability and its oceanic drivers. Clim Dyn 50:4691–4705. https://doi.org/10.1007/s00382-017-3898-0

Li JP, Zheng F, Sun C et al (2019) Pathways of influence of the Northern Hemisphere mid-high latitudes on East Asian climate: a review. Adv Atmos Sci 36:902–921. https://doi.org/10.1007/s00376-019-8236-5

Li XF, Hu Z-Z, Tseng Y-H et al (2022) A historical perspective of the La Niña Event in 2020/21. J Geophys Res 127:e2021JD035546. https://doi.org/10.1029/2021JD035546

Liebmann B, Smith CA (1996) Description of a complete (interpolated) OLR dataset. Bull Am Meteorol Soc 77:1275–1277

Liu YY, Gao H (2021) Features and possible causes of climate anomalies in China in spring 2021. Meteorol Mon 47:1320–1332 ((in Chinese))

Liu BQ, Zhu CW, Ma SM et al (2022) Combined effects of tropical Indo-Pacific-Atlantic SST anomalies on record-breaking floods over Central-North China in September 2021. J Clim 35:6191–6205. https://doi.org/10.1175/JCLI-D-21-0988.1

Ninomiya K, Muraki H (1986) Large-scale circulations over East Asia during Baiu period of 1979. J Meteorol Soc Jpn 64:409–429. https://doi.org/10.2151/jmsj1965.64.3_409

Qiao SB, Chen D, Wang B et al (2021) The longest 2020 Meiyu season over the past 60 years: subseasonal perspective and its predictions. Geophys Res Lett 48:e2021GL093596. https://doi.org/10.1029/2021GL093596

Ren ZH, Yu Y, Zou FL et al (2012) Quality detection of surface historical basic meteorological data. J Appl Meteorol Sci 23:739–747 ((in Chinese))

Ren HC, Zuo JQ, Li WJ (2017) Role of the North Atlantic SST anomalies in the 1998 and 2016 summer floods in China. Acta Meteorol Sin 75:877–893 ((in Chinese))

Ren HC, Zuo JQ, Li WJ (2021) The impact of tropical Atlantic SST variability on the tropical atmosphere during boreal summer. J Clim 34:6705–6723. https://doi.org/10.1175/JCLI-D-20-0259.1

Reynolds RW, Rayner NA, Smith TM et al (2002) An improved in situ and satellite SST analysis for climate. J Clim 15:1609–1625. https://doi.org/10.1175/1520-0442(2002)015%3c1609:AIISAS%3e2.0.CO;2

Rong XY, Zhang RH, Li T (2010) Impacts of Atlantic sea surface temperature anomalies on Indo-East Asian summer monsoon-ENSO relationship. Chin Sci Bull 55:2458–2468. https://doi.org/10.1007/s11434-010-3098-3

Tao SY, Chen LX (1987) A review of recent research on the East Asian summer monsoon in China. In: Chang CP, Krishnamurti TN (eds) Monsoon meteorology. Oxford University Press, Oxford, pp 60–92

Tao WC, Huang G, Wu RG et al (2017) Asymmetry in summertime atmospheric circulation anomalies over the northwest Pacific during decaying phase of El Niño and La Niña. Clim Dyn 49:2007–2023. https://doi.org/10.1007/s00382-016-3432-9

Wang B (1987) The development mechanism for Tibetan Plateau warm vortices. J Atmos Sci 44:2978–2994

Wang Z, Gao K (2003) Sensitivity experiments of an eastward-moving southwest vortex to initial perturbations. Adv Atmos Sci 20:638–649. https://doi.org/10.1007/BF02915507

Wang B, Wu RG, Fu XH (2000) Pacific-East Asian teleconnection: how does ENSO affect East Asian climate? J Clim 13:1517–1536. https://doi.org/10.1175/1520-0442(2000)013%3c1517:PEATHD%3e2.0.CO;2

Wang B, Xiang B, Lee J-Y (2013) Subtropical high predictability establishes a promising way for monsoon and tropical storm predictions. Proc Natl Acad Sci USA 110:2718–2722. https://doi.org/10.1073/pnas.1214626110

Wang B, Chen G, Liu F (2019a) Diversity of the Madden-Julian Oscillation. Sci Adv 5:eaax0220. https://doi.org/10.1126/sciadv.aax0220

Wang XH, Tim L, Chen MC (2019b) Mechanism for asymmetric atmospheric responses in the western North Pacific to El Niño and La Niña. Clim Dyn 53:3957–3969. https://doi.org/10.1007/s00382-019-04767-4

Wei K, Ouyang C, Duan H et al (2020) Reflections on the catastrophic 2020 Yangtze River Basin flooding in southern China. The Innovation 1:100038. https://doi.org/10.1016/j.xinn.2020.100038

Wheeler MC, Hendon HH (2004) An all-season real-time multivariate MJO Index: development of an index for monitoring and prediction. Mon Weather Rev 132:1917–1932. https://doi.org/10.1175/1520-0493(2004)132%3c1917:AARMMI%3e2.0.CO;2

Wu ZW, Li JP, He JH et al (2006) Occurrence of droughts and floods during the normal monsoons in the mid- and lower reaches of the Yangtze River. Geophys Res Lett 33:L05813. https://doi.org/10.1029/2005GL024487

Wu BY, Zhang RH, Wang B et al (2009) On the association between spring Arctic sea ice concentration and Chinese summer rainfall. Geophys Res Lett 36:L09501. https://doi.org/10.1029/2009GL037299

Wu B, Li T, Zhou TJ (2010) Asymmetry of atmospheric circulation anomalies over the western North Pacific between El Niño and La Niña. J Clim 23:4807–4822. https://doi.org/10.1175/2010JCLI3222.1

Wu B, Zhou TJ, Li T (2017a) Atmospheric dynamic and thermodynamic processes driving the western North Pacific anomalous anticyclone during El Nino. Part I: maintenance mechanisms. J Clim 30:9621–9635. https://doi.org/10.1175/JCLI-D-16-0489.1

Wu B, Zhou TJ, Li T (2017b) Atmospheric dynamic and thermodynamic processes driving the western North Pacific anomalous anticyclone during El Nino. Part II: formation processes. J Clim 30:9637–9650. https://doi.org/10.1175/JCLI-D-16-0495.1

Xiang B, Wang B, Yu W, Xu S (2013) How can anomalous western North Pacific subtropical high intensify in late summer? Geophys Res Lett 40:2349–2354. https://doi.org/10.1002/grl.50431

Xie SP, Hu K, Hafner J et al (2009) Indian Ocean capacitor effect on Indo-western Pacific climate during the summer following El Nino. J Clim 22:730–747. https://doi.org/10.1175/2008JCLI2544.1

Xie SP, Kosaka Y, Du Y et al (2016) Indowestern Pacific Ocean capacitor and coherent climate anomalies in post-ENSO summer: a review. Adv Atmos Sci 33:411–432. https://doi.org/10.1007/s00376-015-5192-6

Xie F, Zhou X, Li JP et al (2018) Effect of the Indo-Pacific Warm Pool on lower stratospheric water vapor and comparison with the effect of the El Niño-Southern Oscillation. J Clim 31:929–943. https://doi.org/10.1175/JCLI-D-17-0575.1

Zhang RH, Zuo ZY (2011) Impact of spring soil moisture on surface energy balance and summer monsoon circulation over East Asia and precipitation in East China. J Clim 24:3309–3322. https://doi.org/10.1175/2011JCLI4084.1

Zhang RH, Sumi A, Kimoto M (1996) Impact of El Nino on the East Asian Monsoon: a diagnostic study of the '86/87 and '91/92 events. J Meteorol Soc Jpn 74:49–62. https://doi.org/10.2151/jmsj1965.74.1_49

Zhang RN, Zhang RH, Zuo ZY (2017) Impact of Eurasian spring snow decrement on East Asian summer precipitation. J Clim 30:3421–3437. https://doi.org/10.1175/JCLI-D-16-0214.1

Zhang QY, Xuan SL, Sun SQ (2018) Anomalous circulation characteristics of intraseasonal variation of East Asian subtropical westerly jet in summer and precursory signals. Chin J Atmos Sci 42:935–950. https://doi.org/10.3878/j.issn.1006-9895.1803.18107. (**(in Chinese)**)

Zhang WJ, Huang ZC, Jiang F et al (2021) Exceptionally persistent Madden-Julian Oscillation activity contributes to the extreme 2020 East Asian summer monsoon rainfall. Geophys Res Lett 48:e2020GL091588. https://doi.org/10.1029/2020GL091588

Zhao JH, Chen LJ, Wang DQ (2018a) Characteristics and causes analysis of abnormal meiyu in China in 2016. Chin J Atmos Sci 42:1055–1066. https://doi.org/10.3878/j.issn.1006-9895.1708.17170. (**(in Chinese)**)

Zhao JH, Chen LJ, Xiong KG (2018b) Climate characteristics and influential systems of Meiyu to the south of the Yangtze River based on the new monitoring rules. Acta Mereorol Sin 76:680–698. https://doi.org/10.11676/qxxb2018b.025. (**(in Chinese)**)

Zhao JH, Zhang H, Zuo JQ et al (2021) What drives the super strong precipitation over the Yangtze-Huaihe River Basin in the Meiyu period of 2020? Chin J Atmos Sci 45:1433–1450. https://doi.org/10.3878/j.issn.1006-9895.2104.21011. (**(in Chinese)**)

Zhao JH, Chen LJ, Zhang DQ (2022a) Characteristics and causes for the climate anomalies over China in summer 2021. Meteorol Mon 48:107–121 (**(in Chinese)**)

Zhao JH, Zhang H, Zuo JQ et al (2022b) Oceanic drivers and empirical prediction of late summer rainfall variability over Northeast China. Clim Dyn 58:861–878. https://doi.org/10.1007/s00382-021-05945-z

Zuo JQ, Li WJ, Sun CH et al (2019) Remote forcing of the northern tropical Atlantic SST anomalies on the western North Pacific anomalous anticyclone. Clim Dyn 52:2837–2853. https://doi.org/10.1007/s00382-018-4298-9

Zuo JQ, Sun CH, Li WJ et al (2020) Representation of the boreal summer tropical Atlantic–western North Pacifc teleconnection in AGCMs: comparison of CMIP5 and CMIP6. Clim Dyn 55:3025–3041. https://doi.org/10.1007/s00382-020-05427-8